Sustainable Chemical Engineering
http://ojs.wiserpub.com/index.php/SCE/

UNIVERSAL WISER PUBLISHER

Research Article

Enhanced Biodiesel Production from Waste Cooking Oil Using Potash-Enriched Natural Base Catalyst

U. P. Patil[1*], **S. U. Patil**[2]

[1]Department of Chemistry, ACS College, Palus, MS, India
[2]Department of Life Sciences, KRP Kanya Mahavidyalaya, Islampur, MS, India
E-mail: uppatil4143@rediffmail.com

Received: 18 April 2024; **Revised:** 9 May 2024; **Accepted:** 14 May 2024

Graphical Abstract

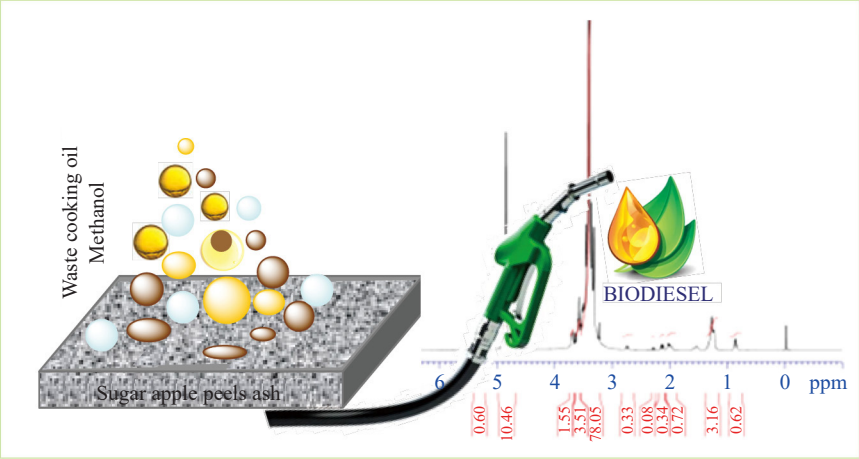

Abstract: The transesterification reaction of waste cooking oil with methanol using a sugar apple peel ash catalyst has been reported. Under optimized conditions, the reaction of the oil with methanol in a molar ratio of 1:10, in the presence of a catalyst (2 g) at 60 °C temperature offered a 94.5% yield of biodiesel within 120 min. The heterogeneous catalyst was developed via a straightforward calcination process using fruit processing industry waste peels of sugar apples. The characterization of the catalyst by FTIR, EDS, SEM, XRD, N_2 sorption, and XRF analysis revealed a higher concentration of potassium species which is possibly responsible for the promotion of the transesterification reaction more efficiently. This approach offers cost competitiveness, reusability of the catalyst, simplicity of operation, and high biodiesel yields. This study underscores the potential of utilizing waste materials for sustainable biodiesel production, contributing to environmental preservation and economic viability.

***Keywords*:** waste cooking oil, heterogeneous catalyst, sugar apple peel ash, biodiesel

DOI: https://doi.org/10.37256/sce.5220244778

1. Introduction

Diesel fuel is typically made from crude oil through a refining process. It consists of hydrocarbon chains, which are longer and heavier compared to those found in gasoline. The exact composition and properties of diesel fuel can vary depending on factors such as the source of crude oil and the refining methods used. Diesel fuel offers several advantages, including better fuel efficiency, higher torque output, and longer engine life.[1] Because of these inherent properties of diesel, it has been consumed on a large scale. The utilization of non-renewable and conventional energy sources is dominant worldwide. World energy consumption doubled between 1971 and 2001 and the demand for energy will increase by 53% by the year 2030.[2]

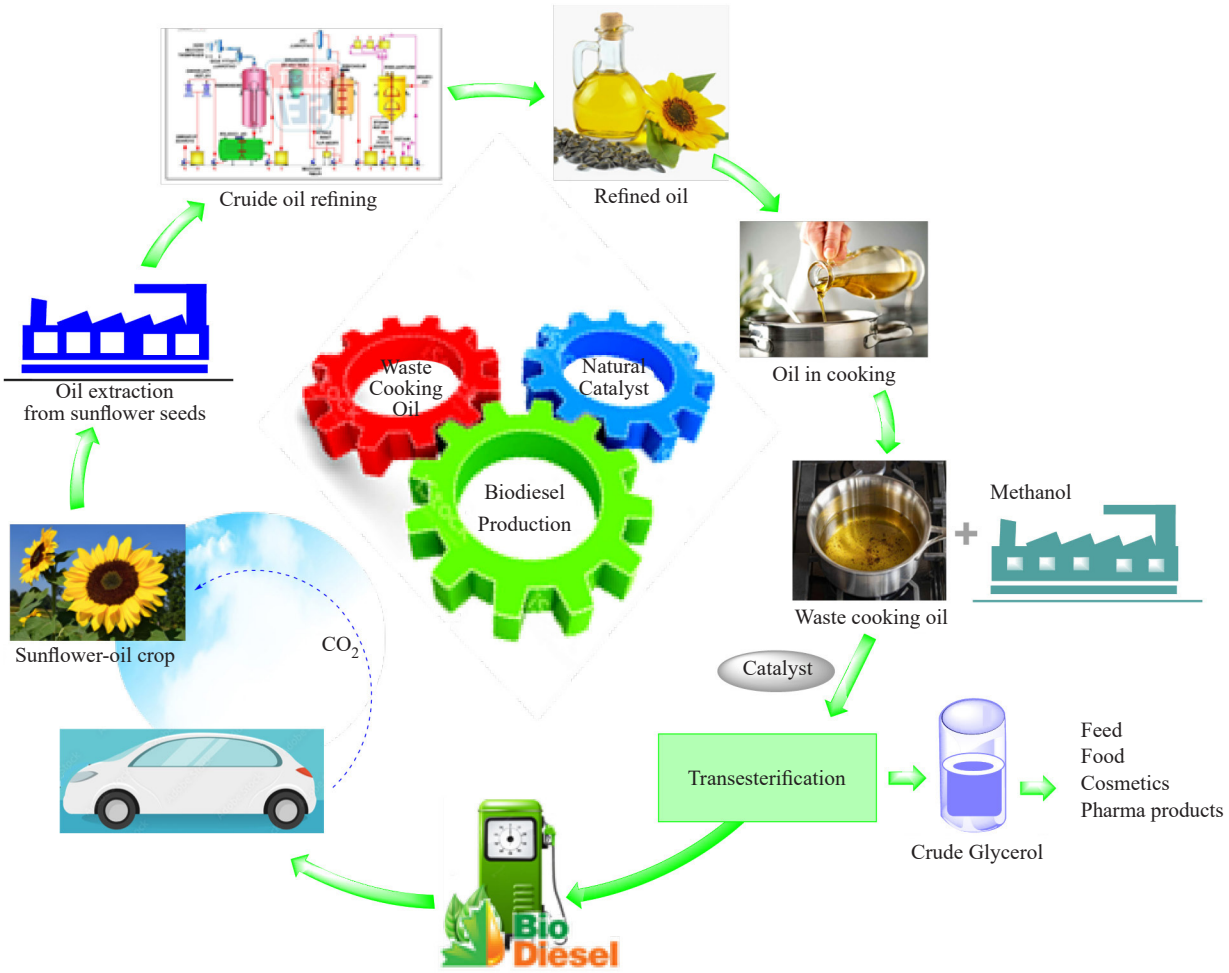

Figure 1. Overall biodiesel production process and its applications

However, depletion in reservoirs, skyrocketing prices, and price instability of fossil crude oil are considered serious threats to economically backward nations. Besides, diesel fuel has traditionally been associated with higher emissions of pollutants and particulate matter. The large-scale greenhouse gas emission from fossil fuels is responsible for global warming.[3] In this context, biodiesel is currently one of the promising alternatives to fossil fuel diesel which is obtained from vegetable oils or animal fats via a transesterification process using methanol or ethanol or a mixture of both using suitable catalysts (Figure 1). Biodiesel fuel offers several advantages, including better fuel efficiency, higher torque output, and longer engine life. It has lower greenhouse gas emissions compared to diesel.[4] It reduces CO_2 emissions by

up to 86% and it has significantly lower levels of particulate matter, oxides of N, and S, and other harmful pollutants.[5] The use of biodiesel helps to mitigate climate change and improve air quality. It is derived from renewable feedstock, which can be replenished through agricultural practices. Biodiesel offers a sustainable energy option and reduces dependence on fossil fuel imports. By utilizing domestic resources, nations can enhance their energy security and reduce vulnerability to fluctuations in oil prices or supply distributions.[6]

Biodiesel production creates jobs in agriculture, feedstock production, and the biofuel industry. It can stimulate rural economies by providing new markets for farmers and promoting local industries. Additionally, biodiesel production can contribute to energy independence and reduce trade deficits associated with petroleum imports.[7] Biodiesel can be blended with petroleum diesel and used in existing diesel engines without requiring significant modifications or infrastructure changes. It can be used in various applications, including transportation, power generation, and heating. This compatibility makes it easier to integrate biodiesel into existing fuel distribution systems.[8]

Biodiesel can be produced from recycled cooking oils and waste fats, reducing waste disposal and promoting recycling efforts. It provides a valuable outlet for these waste materials and reduces environmental pollution.[9] Biodiesel feedstock, such as soybeans, peanuts, canola, palm oil, and other oil seeds can create additional markets for farmers. The cultivation of these crops can help diversify agricultural production, improve rural incomes, and support sustainable farming practices.[10] Overall; biodiesel offers a range of important benefits, including environmental sustainability, energy security, economic growth, waste reduction, and agricultural opportunities. By promoting the use of biodiesel, we can move towards a more sustainable and greener future.

In the transesterification process, heterogeneous catalysts are favored due to their ease of separation and purification, as well as their non-corrosive nature and recyclability. This catalytic system offers advantages in terms of both operational efficiency and environmental impact. By utilizing natural feedstock materials for creating heterogeneous catalysts, the process becomes more economical and environmentally friendly. It reduces dependency on synthetic or non-renewable resources, aligning with sustainability goals. Furthermore, catalysts derived from natural sources often exhibit desirable properties, such as high activity and selectivity, enhancing the overall efficiency of the transesterification reaction.[11-13]

Due to economic and environmental benefits, in recent years, biodiesel has attracted significant attention from researchers, the scientific community, governments, and industries. In this regard, hard efforts have been taken by the scientific community and industry to design and develop sustainable green methods to produce an alternative fuel to fossil fuel. A good number of methods have been reported in the literature for biodiesel production from various natural sources using acid/base catalysts. R. Selaimia et al.[14] have produced biodiesel from vegetable oil using a KOH catalyst. In another study, Yusuff and co-workers[15] prepared biodiesel from waste cooking oil using a zinc-modified anthill catalyst that offered 83.16% of biodiesel. In another report, Ahmad et al.[16] synthesized biodiesel from the non-edible seed oil of *Cichorium intybus* using a MgO catalyst that afforded a 95% yield of biodiesel. Degfie et al.[17] synthesized a nano-catalyst CaO and employed it for the transesterification reaction of methanol and waste cooking oil which gave 96% yield of biodiesel. Park and co-workers[18] synthesized biodiesel from locally sourced restaurant waste cooking oil and grease via transesterification reaction with methanol using NaOH catalyst at 65 °C temperature for 2.5 h under reflux.

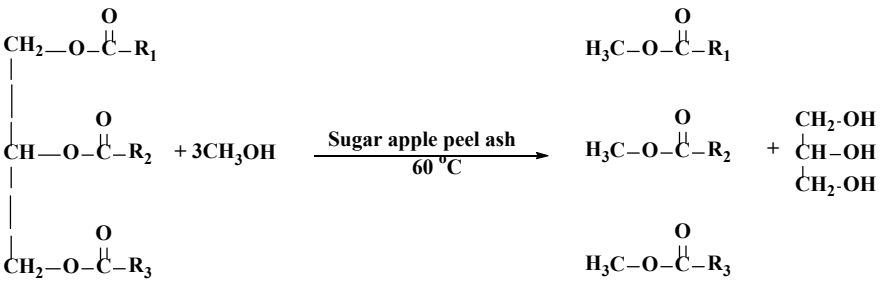

Figure 2. Synthesis of biodiesel using sugar apple peel ash catalyst

Exponentially, several methods have been reported using synthetic as well as naturally sourced acid/base catalysis since the last decade. However, many methods have certain drawbacks such as the use of synthetic acids/bases which are hazardous and not environmentally friendly, poor yield, no or least catalytic reusability, leaching of active sites from catalysts like CaO, and others. From the green chemistry perspective, the use of waste material as a precursor and waste-derived catalytic material with excellent yield of the product is always desirable. With this view, and based on our previous work on the utilization of waste-derived catalysts in the organic transformations,[19-25] we have developed a simple, novel, economical, and environmentally benign method for biodiesel production (Figure 2) from waste cooking oil using industrial waste sugar apple peel ash catalyst at 60 °C that offered 94.5% yield of biodiesel. Therefore, the present protocol enhances green credentials and could be suitable for large-scale production of biodiesel.

2. Experimental

2.1 *Materials*

The sample of waste cooking oil was collected from the college canteen located on the campus of Arts, Commerce and Science College, Palus Dist: Sangli (MS, India). The collected waste oil sample was filtered to remove food debris and other impurities. All essential chemicals were purchased from Loba Chemie and used as received without further purification. N_2 adsorption-desorption isotherm was obtained using NOVA1000e Quantachrome, USA instrument. FT-IR spectra were recorded on Bruker (Alpha 100508, USA), and wave numbers ($\tilde{\upsilon}$) were reported in cm^{-1}. ^{1}H and ^{13}C-NMR spectra of compounds were recorded on AVANCE-300 spectrometer (Bruker, USA). Chemical shifts (δ) introduced in parts per million (ppm) using the residue solvent peaks as a reference relative to TMS. Pre-coated plates of Silica gel 60 F254 were used for thin-layer chromatography (TLC). Powder XRD measurement recorded on XPERT-PRO X-Ray Powder Diffractometer (PANalytical, Pretoria, S.A.) using Cu Kα radiation (λ = 1.5406Å) with scattering angle (2 theta). The microscopic morphology was examined by JEOL 6380A (Japan) Scanning electron microscopy (SEM). EDS analysis was performed using an EDS: Bruker XFlash 6|30 microscope with excellent energy resolution (123 eV at Mn Kα and 453V at C Kα) and element detection range from 4 Be to 95 Am (Bruker, USA). The XRF analysis was carried out using X-Ray Fluorescence spectrometer (PANanlytical, USA).

2.2 *Catalyst preparation*

The plant *Annona squamosa L.* (family: *Annonaceae*) is generally known as a sugar apple or custard apple. It is a common plant, and its species are found in the US, Indonesia, the West Indies, Thailand, Taiwan, southern Asia, Brazil, and many more countries.[26] The species of this plant are cultivated as a commercial fruit tree. In India, its local names are aatoa, amritaphala, athichakku, seethapalam, seethaphala, sharifa, and sitaphal.[27] The sugar apple fruit (100 g) is composed of water (73.22 g), energy (101 kcal), protein (3.0 g), carbohydrates (235.20 g), total dietary fibers (2.4 g), total fat (0.29 g), ash (0.77 g), and minerals such as Ca (24 mg), Mg (21 mg), K (382 mg), P (32 mg), Na (3 mg), Fe (0.60 mg), Se (0.60 mg), Cu (0.086 mg), Zn (0.10 mg). The vitamins C (ascorbic acid) (19 mg), vitamin B_1, B_2, B_3, B_5, B_6, B_9 and vitamin A in minor amounts are present in the fruit.[28-29]

Venkatesh Farm in Walwa, Maharashtra, India operates as a small-scale fruit processing industry. Post-processing, the facility generates a weekly waste output ranging from 600 kg to 1,200 kg. Fresh peels of sugar apple (*Annona squamosa*) were collected from the Venkatesh Farm. The collected peels were washed with distilled water, dried in the sun, cut into small pieces, and completely burnt in the open air. The obtained ash was ground to fine powder, and it was used as a catalyst (Figure 3). Dry peels calcined in the muffle furnace exhibited almost the same catalytic activity. The catalyst was characterized by FT-IR, XRF, XRD, SEM, EDS, BET, and DSC-TGA analytical techniques.

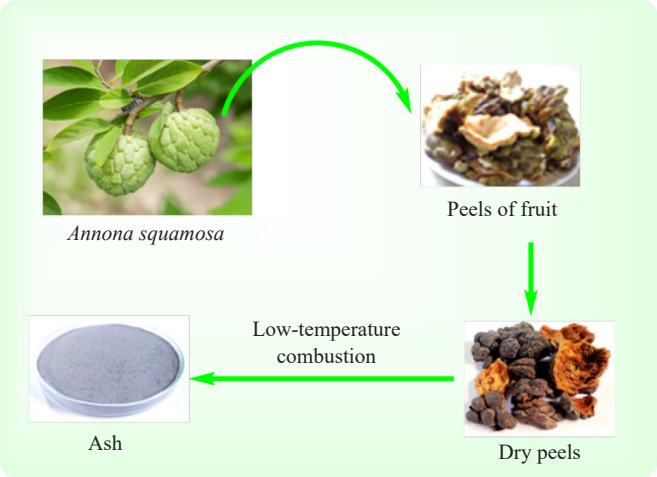

Figure 3. Preparation of the sugar apple peels ash catalyst

2.3 *Catalyst characterization*

The XRF (Pananalytical, USA) analysis exhibited that the main components of the sugar apple peel ash were K_2O (52.65%), P_2O_5 (12.55%), MgO (15.26%), and CaO (8.67%) while Fe_2O_3, Al_2O_3, MnO and NaO constituted the remaining ash (Table 1). The XRF analysis showed that the sugar apple peel ash contains potassium oxide in a higher concentration.

Table 1. XRF analysis of sugar apple peels ash

Sr. No.	Constituents	Concentration (%)
1	K_2O	52.65
2	P_2O_5	12.55
3	MgO	15.26
4	CaO	8.67
5	Cl	3.44
6	S	1.85
7	Fe_2O_3	4.43
8	Al_2O_3	1.12
9	Na_2O	0.010
10	SiO_2	0.001
11	CuO	0.01

The FT-IR (Bruker, ALPHA 100508, US) spectral analysis (Figure 4) of the catalyst exhibited the characteristic bands observed in the region of 1,751 cm^{-1} is assigned to the C-O group, which possibly because of the presence of metal carbonates. The absorption band at 1,485 cm^{-1} is assigned to O-H, while the strong peak in the region of 1,383 and 593 cm^{-1} is ascribed to the K_2CO_3. The peaks at 1,114, 1,043 and 863 cm^{-1} can be attributed to the metal oxides. FT-IR absorption spectra highlight the presence of metal hydroxides and carbonates in the sugar apple peel ash catalyst.

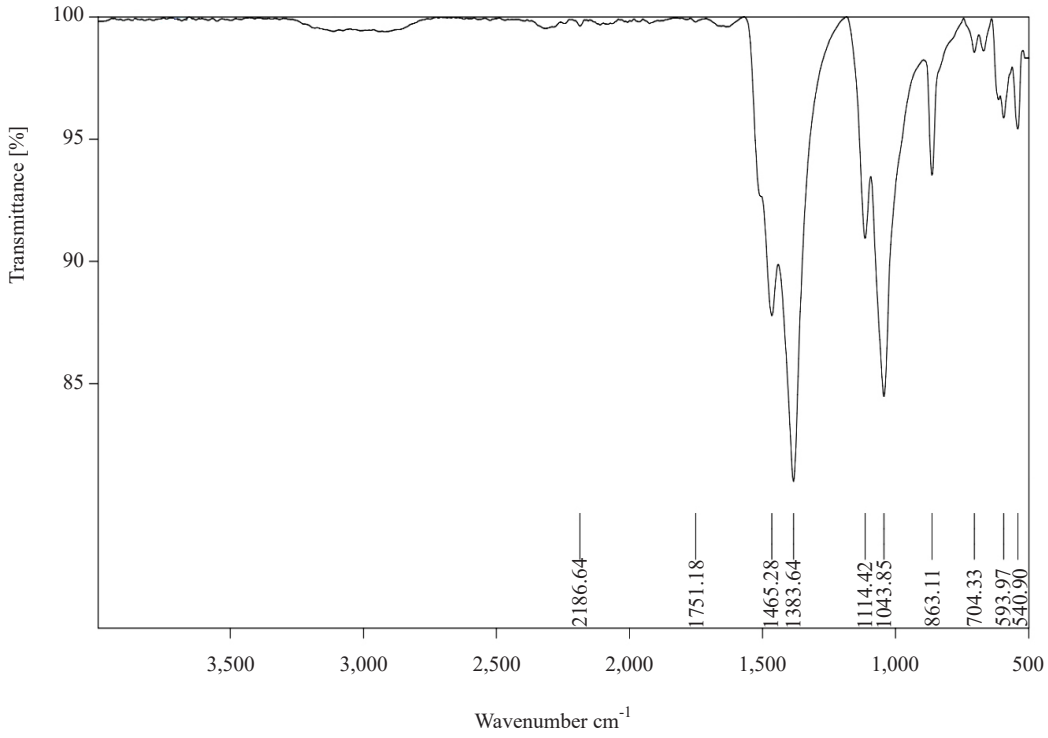

Figure 4. FTIR spectrum of sugar apple peels ash

Powder XRD measurement recorded on XPERT-PRO X-Ray Powder Diffractometer (PANalytical, Pretoria, S.A.) using Cu Kα radiation (λ = 1.5406Å) with scattering angle (2 theta). The XRD pattern exhibited the presence of the metal oxides and carbonates in the sugar apple peel ash catalyst (Figure 5). The intense peaks of K_2O and K_2CO_3 were observed at 2θ = 26.64°, 28.34°, 29.78°, and 40.48° (JCPDS File No. 77-2176, 47-1701, 87-0730). The peak at 44.89° attributed to MgO (JCPDS File No. 04-0829, 75-1525), the peak at 2θ = 30.30° correspond to CaO and $CaCO_3$ (JCPDS File No. 87-1863 and 82-1691). The peak of P_2O_5 was observed at 43.32° (JCPDS File No. 5-0488). In addition, another peak was observed at 2θ = 25.86° (JCPDS File No. 89-2810) attributed to Fe_2O_3. Hence, the XRD pattern of sugar apple peel ash also underlined the crystalline nature of the ash and the presence of alkali and alkaline earth metals in the catalyst. The crystallite size of the sugar apple ash based on the two peaks (26.64° and 30.30°) is 45.37 and 21.50 nm, with an average crystal size of 33.43 nm.[30]

The microscopic morphology of the sugar apple peel ash was examined by JEOL 6380A (Japan) Scanning electron microscopy (SEM) (Figure 6). It showed irregular particles with heterogeneous morphology. The ash particles have irregular cavities, porous surfaces with smooth edges, agglomerated and flower-like appearance. Material with this type of morphology generally has a high specific surface area which provides good absorption capacity. This type of nature of peel ash facilitates organic transformation very smoothly and effectively.

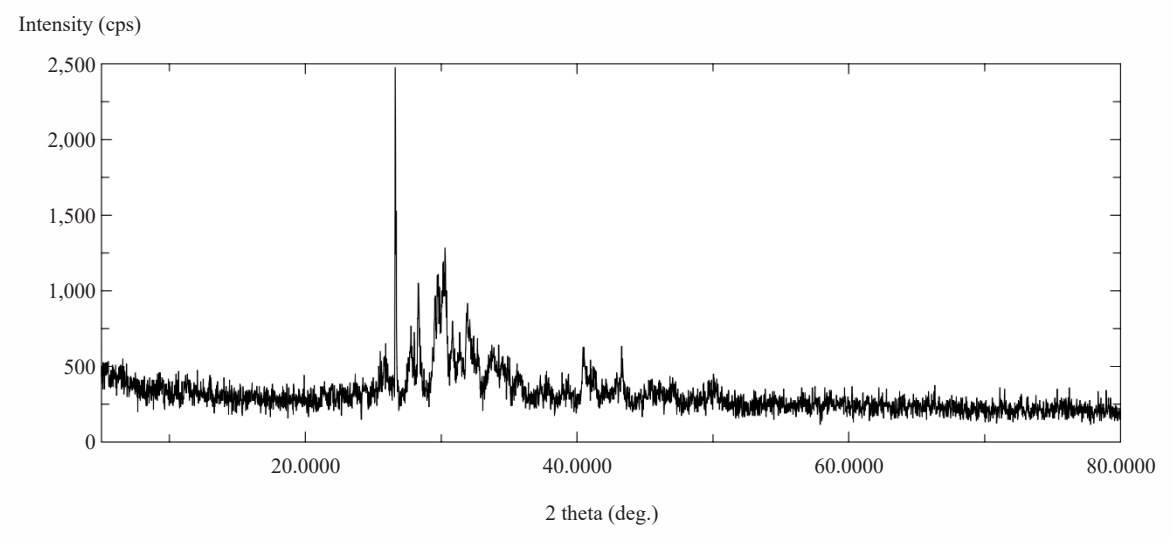

Figure 5 XRD pattern of sugar apple peels ash

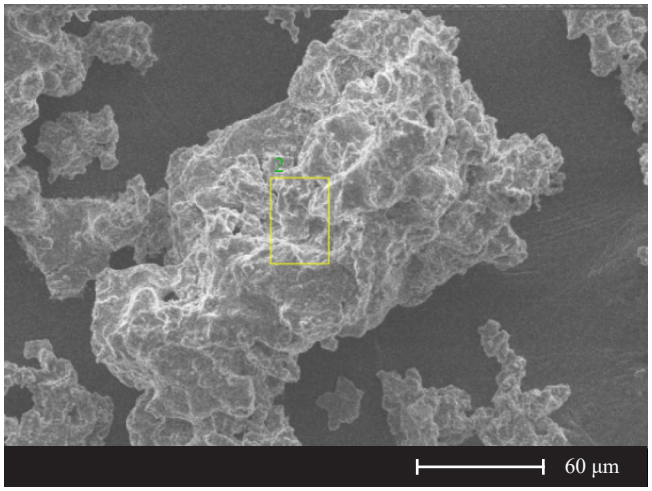

Figure 6. SEM image of sugar apple peels ash

The energy-dispersive X-ray spectroscopy (EDS) was performed using EDS: Bruker XFlash 6|30 (USA). The EDX spectrum of peel ash is depicted in Figure 7. The EDX analysis of peel ash has shown that K (66.09%) is a major constituent, while Al (0.90%) and Mg (0.78%) are minor constituents in the catalyst. It supports the presence of basic active sites in the catalyst.

Thermogravimetric analysis of sugar apple peel powder was carried out to examine the thermal stability. DSC-TGA curves of peel powder are depicted in Figure 8.

As per the obtained thermogram, it is clear that the thermal degradation of peel powder occurred in three steps. Initially, moisture was evaporated from the peel powder. In the next level, at 536.82 °C temperature, hemicellulose, cellulose, and lignin were decomposed. The mass of the sample was reduced vastly in the range of 184.71 °C to 537.01 °C temperature. There was a loss in weight at 184.71 °C, 361.27 °C, and 537.01 °C due to the decomposition of organic components in the peels powder. The decomposition of sugar apple peel powder after 537.01 °C was not observed in the graph, which indicates the remaining part of the sample contains minerals in the form of oxides, carbonates, or other salts in higher concentrations.

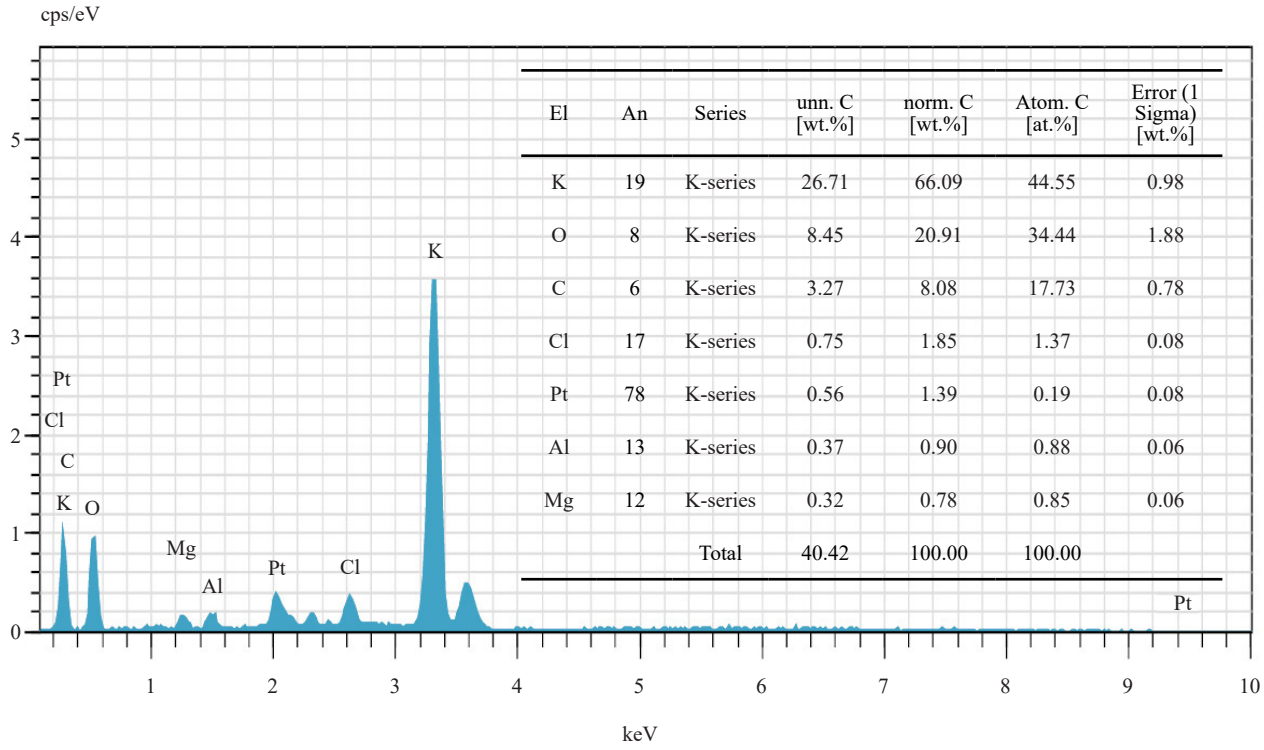

Figure 7. EDX analysis of sugar apple peels ash

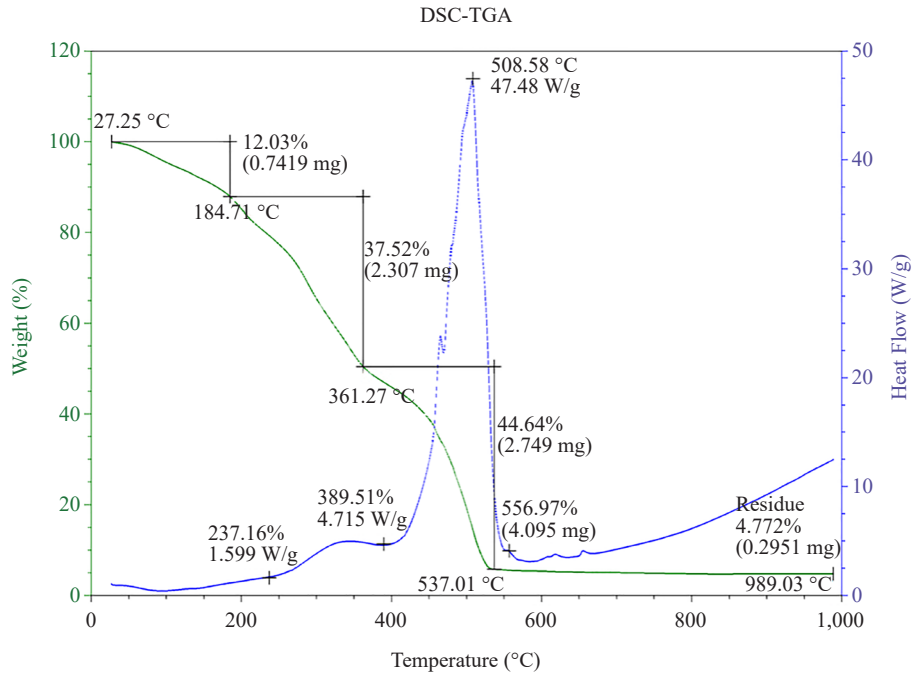

Figure 8. DSC-TGA thermogram of the sugar apple peels powder

N_2 adsorption-desorption isotherm (Figure 9) of a catalyst belongs to the Type-IV (as per IUPAC classification)

with a typical H3 hysteresis loop, highlighting the mesoporous nature of the catalyst. The textural data is given in Table 2. The mesoporous nature, high surface area, and porous skeleton of the catalyst promote transesterification reaction more efficiently.

Table 2. Textural properties of the sugar apple peels ash

Sample	Surface area	Pore volume	Pore diameter
Sugar apple peels ash	9.205 m^2/g	0.022 cc/g	1.810 nm

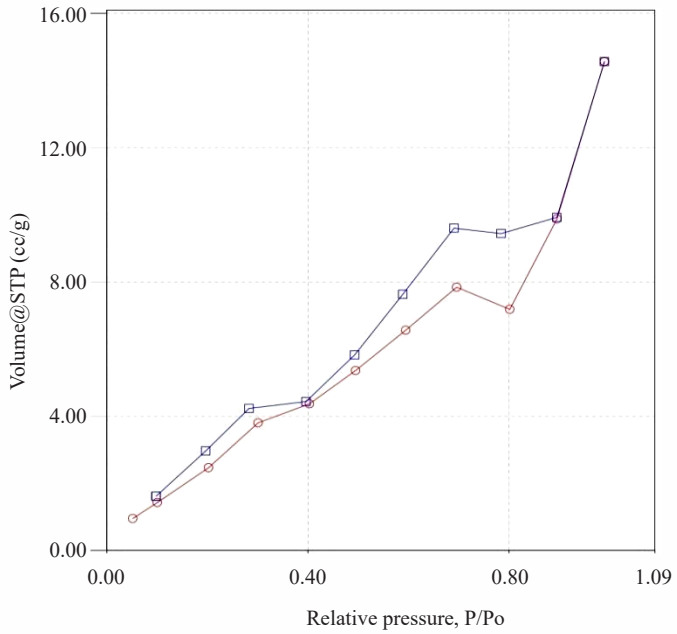

Figure 9. N_2 adsorption-desorption isotherm of sugar apple peels ash catalyst

Table 3. Hammett indicators used for the measurement of basic strength of sugar apple peel ash

Entry	Indicators	Original color	Basic color	Base strength	Color change
1	Phenolphthalein	Colorless	Pink	H_ = 9.8	Pink
2	Alizarin yellow R	Yellow	Red	H_ = 11	Red
3	2,3,4-trinitroaniline	Yellow	Reddish-orange	H_ = 12.2	Reddish-orange
4	2,4-dinitroaniline	Yellow	Violet	H_ = 15	No color change

The catalyst's surface basic strength was analyzed using the Hammett indicator method[31] with phenolphthalein (H_ = 9.8), alizarin yellow R (H_ = 11), 2,4,6-trinitroaniline (H_ = 12.2), and 2,4-dinitroaniline (H_ = 15) indicators (Table 3). For each trial, 2 mL of the Hammett indicator solution in benzene was added to 200 mg of the catalyst. The results

indicated significant color changes with the first three indicators, while the fourth indicator showed no discernible color change. This suggests that the basic strength of the catalyst likely falls within the range of $11 \leq H\_ \leq 12.2$.

2.4 *Synthesis of biodiesel*

Waste cooking oil collected from the college canteen was filtered to remove solid impurities. Oil-free from impurities was then heated above 100 °C temperature to remove water. A 250 mL round bottom flask was charged with 10 mL of filtered cooking oil. The mixture of methanol (100 mL) and sugar apple peel ash (2 g) was added to the oil and the resulting mixture was stirred at 60 °C temperature for 2 h. After completion of the reaction, the reaction mixture was kept at room temperature for 12 h. It was then filtered. The filtrate was transferred to a separating funnel. After the formation of two layers of biodiesel and glycerol, both were separated and stored in bottles. Biodiesel was further washed and dried. It was then characterized by analytical tools.

3. Result and discussion

In our pursuit of biodiesel production, we've undertaken numerous trial reactions involving waste cooking oil and methanol, experimenting with varying molar ratios, catalyst quantities, and temperature conditions. Impressively, when we combined waste cooking oil with methanol at a 1:10 molar ratio, utilized 2 grams of sugar apple peel ash catalyst, and maintained a temperature of 60 °C, we achieved a remarkable biodiesel yield of 94.5%. Moreover, subsequent increases in molar ratios (oil to methanol), catalyst amounts, and temperature failed to enhance the biodiesel production yield. Following the optimization of these reaction conditions, we subjected the resultant pure biodiesel to thorough characterization using a diverse array of analytical methods.

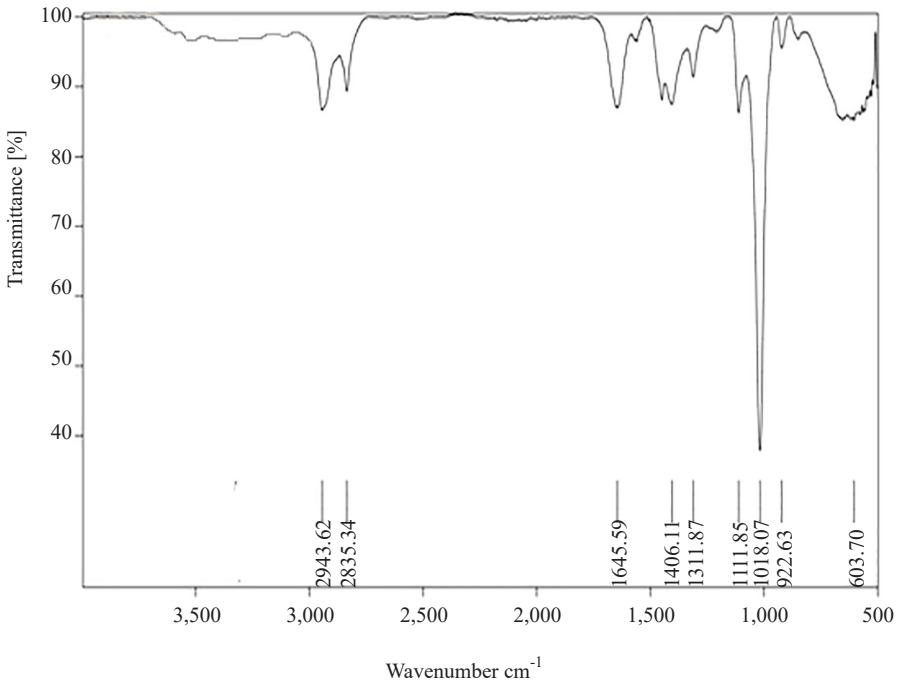

Figure 10. FTIR spectra of biodiesel

FTIR spectra of biodiesel have been shown in Figure 10. The peak at 2,943 cm^{-1} is ascribed to the Csp^2-H of the

vinyl hydrogen, and a peak at 2,835 cm^{-1} corresponds to Csp^3-H_2 symmetric stretching modes. An intensive peak at 1,645 cm^{-1} is associated with C = O stretch of the ester, while a low-intensity peak at 1,595 cm^{-1} is assigned to the C = C of alkene. The peak at 1,406 cm^{-1} is prescribed to Csp^3-H_2 bending mode, and a peak at 1,311 cm^{-1} is associated with Csp^3-H_3 bending mode while the peak at 803 corresponds to Csp^3-H_2. From the data, it is clear that highly pure biodiesel is formed from waste cooking oil. In addition, peaks are not observed in the 3,000 cm^{-1} to 3,500 cm^{-1} region indicating that synthesized biodiesel is free from water.

The ^{1}H-NMR spectrum of the synthesized biodiesel is depicted in Figure 11. In the ^{1}H-NMR spectrum, the characteristic peaks of -OCH_3 protons as a singlet at 3.672 ppm and methylene protons as a triplet at 2.346 ppm were observed.

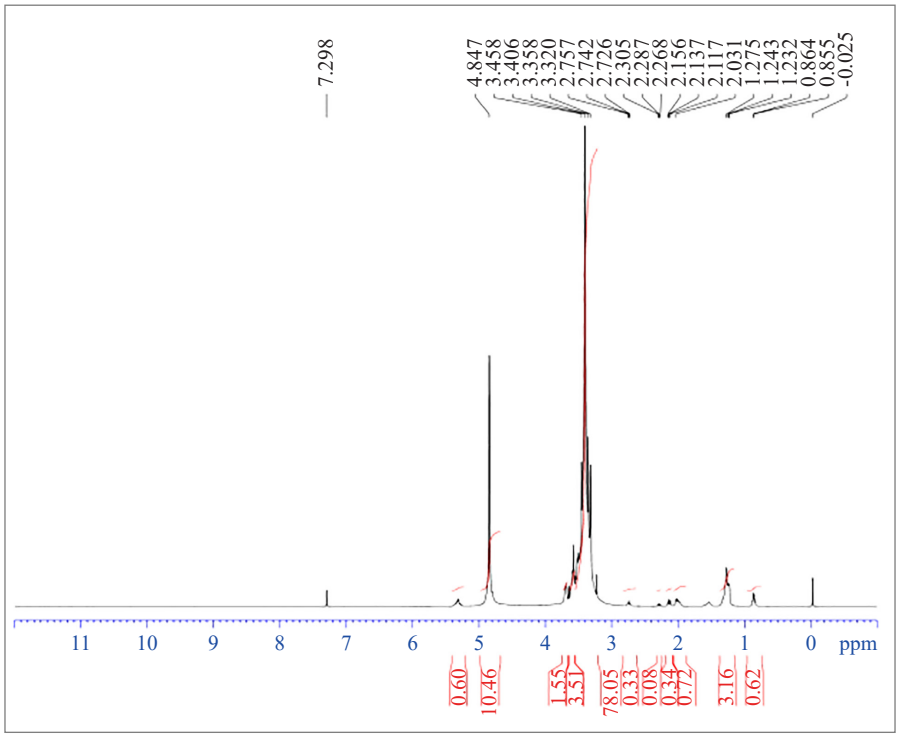

Figure 11. ^{1}H-NMR spectrum of the biodiesel

These two peaks are the distinct peaks for the confirmation of the methyl esters in biodiesel. Moreover, the peaks observed at 0.891 ppm is associated with terminal methyl protons, a strong signal at 1.291 ppm assigned to the methylene protons of the carbon chain, while a multiplet at 1.623 ppm ascribed to β-carbonyl methylene protons, and a signal at 5.321 ppm due to olefinic hydrogen.

The yield of the biodiesel was calculated by using the equation:

$$\%\ yield\ of\ Biodiesel = \frac{Grams\ of\ biodiesel\ produced}{Grams\ of\ oil\ used} \times 100 \quad (1)$$

The % yield of biodiesel was calculated using Equation 1. It was found to be 94.5%.

The ^{13}C-NMR spectrum of the biodiesel is shown in Figure 12. The characteristic peaks at 182.4 ppm and 49.8 ppm are associated with ester carbonyl (-COO-) and C-O, respectively. The peaks at 132.4 and 127.8 ppm indicated the unsaturation in methyl esters. Moreover, a peak at 62.8 ppm is ascribed to -CH_2 = CH = CH_2-. While, the peaks in the range of 34.0 to 28.9 ppm correspond to aliphatic $(CH_2)_n$- carbon, and the peak at 13.8 ppm is due to terminal -CH_3

group carbon.

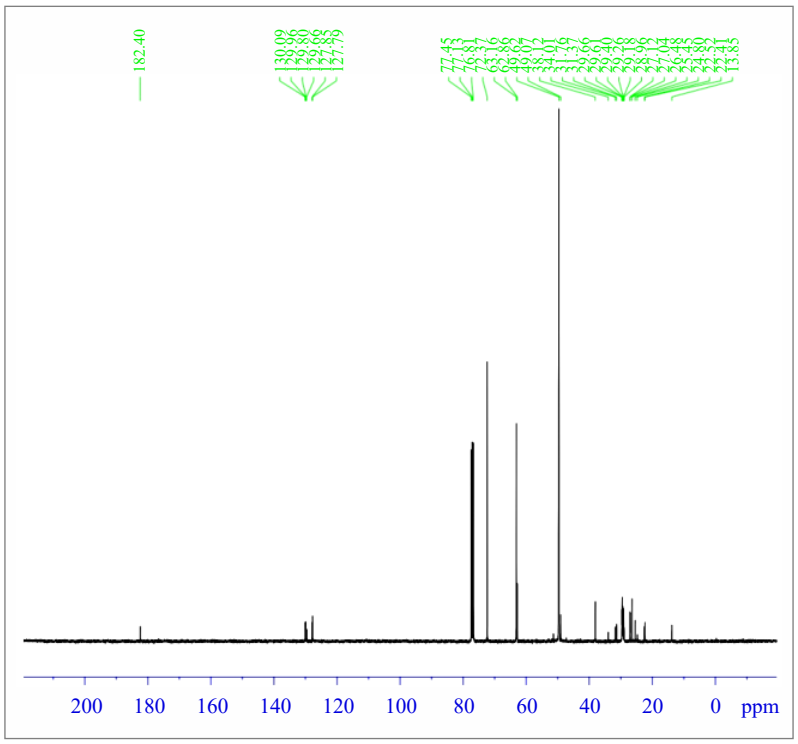

Figure 12. ^{13}C-NMR spectrum of the biodiesel

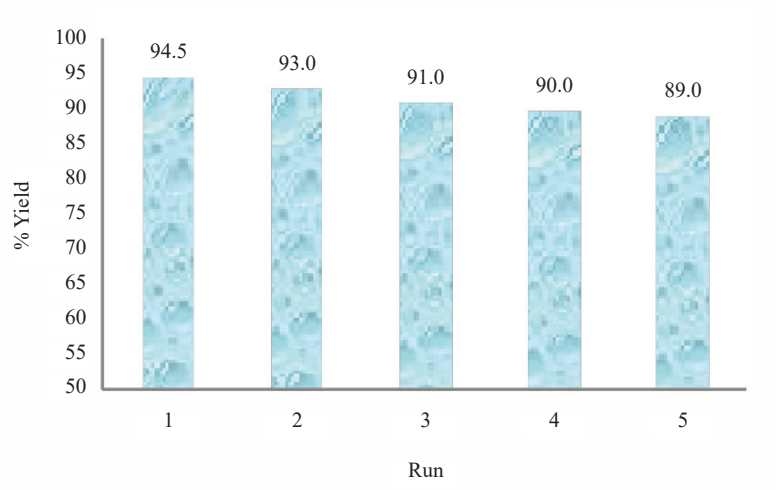

Figure 13. Reusability of the sugar apple peels ash catalyst in biodiesel production

From the green chemistry perspective, it is highly essential to test the reusability of the catalyst. A reusable catalyst is always desirable because it reduces waste and the cost of the product. With this view, we have reused the catalyst for five times in the transesterification reaction of waste cooking oil with methanol in a molar ratio 1:10 using sugar apple peel ash catalyst (2 g) at 60 °C (Figure 13). After each run, the catalyst was separated, washed with methanol and dried

at 100 °C for 2 h. After the 5th run, 89% yield of the biodiesel was obtained. A slight reduction in the yield may be due to the leaching of active metals and or catalytic surface deactivation because of impurities. The recovered catalyst was characterized by SEM and EDS analysis after the 5th run. The SEM image (Figure 14) revealed the particles exhibited a spherical shape and were agglomerated. Additionally, EDS analysis (Figure 15) indicated a slight reduction in K species (61.60%).

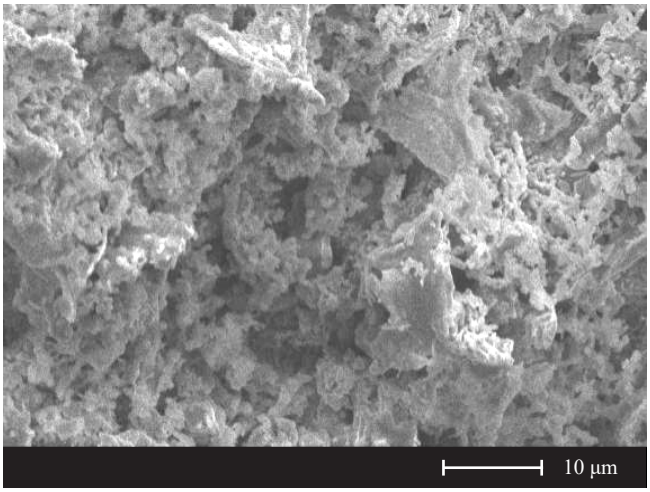

Figure 14. SEM micrograph of the catalyst after 5th run.

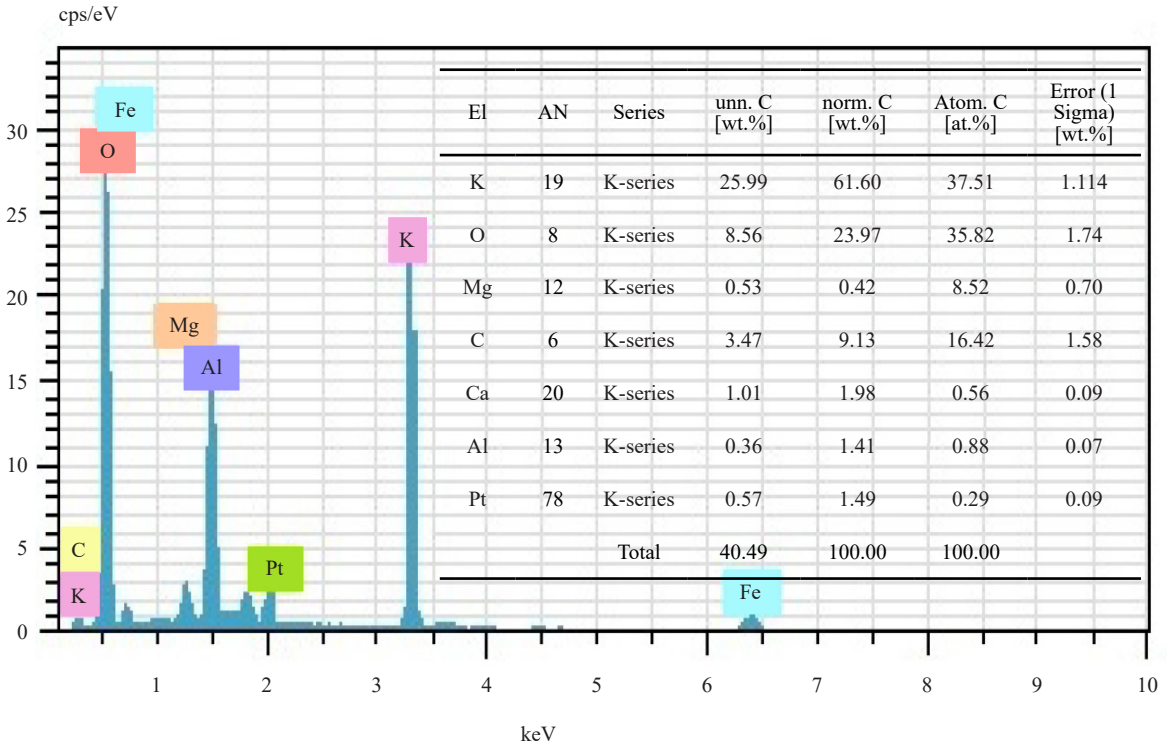

El	AN	Series	unn. C [wt.%]	norm. C [wt.%]	Atom. C [at.%]	Error (1 Sigma) [wt.%]
K	19	K-series	25.99	61.60	37.51	1.114
O	8	K-series	8.56	23.97	35.82	1.74
Mg	12	K-series	0.53	0.42	8.52	0.70
C	6	K-series	3.47	9.13	16.42	1.58
Ca	20	K-series	1.01	1.98	0.56	0.09
Al	13	K-series	0.36	1.41	0.88	0.07
Pt	78	K-series	0.57	1.49	0.29	0.09
		Total	40.49	100.00	100.00	

Figure 15. EDS analysis of the catalyst after 5th run

One of the main reasons for the deactivation of heterogeneous catalysts in the transesterification process is the leaching of active sites into the reaction medium. To investigate the impact of active metals leaching, we conducted a leaching test by removing the catalyst from the reaction mixture after 30 min. and stirring the reaction mixture under optimized conditions for 4 h. However, we couldn't detect any product, which suggests that the active metal sites were not leached out from the catalyst.

4. Conclusion

In conclusion, we have developed a very simple efficient and novel method for the synthesis of biodiesel from waste cooking oil using industrial waste sugar apple peel ash catalyst. From the spectral analysis, it is clear that highly pure biodiesel has been obtained from waste cooking oil with good yield. The striking features of this protocol include the use of waste cooking oil instead of edible oil, industry waste derived catalysts therefore cost-effective and good yield of the biodiesel.

Acknowledgment

The authors express their gratitude to Shivaji University, Kolhapur, Arts, Commerce, and Science College, Palus, as well as KRP Kanya Mahavidyalaya, Islampur, for their generous support and provision of necessary facilities.

Conflict of interest

The authors declare no competing financial interest.

References

[1] Gad, S. C. Diesel Fuel. In *Encyclopedia of Toxicology*; Wexler, P., Ed.; Elsevier, 2005; pp 19-22.
[2] Selaimia, R.; Beghiel, A.; Oumeddour, R. *Procedia Soc. Behav. Sci.* **2015,** *195*, 1633-1638.
[3] Roy, M. M.; Wang, W.; Bujold, J. *Appl. Energy* **2013,** *106*, 198-208.
[4] Boretti, A. *Front. Mech. Eng.* **2019,** *6*, 493925.
[5] Xu, H.; Ou, L.; Li, Y.; Hawkins, T. R.; Wang, M. *Environ. Sci. Technol*. **2022,** *56*, 7512-7521.
[6] Yaakob, Z.; Mohammad, M.; Alherbawi, M.; Alam, Z.; Sopian, K. *Renew. Sustain. Energy Rev*. **2013,** *18*, 184-193.
[7] Sani, Y. M.; Daud, W. M. A. W.; Abdul Aziz, A. R. Biodiesel feedstock and production technologies: Successes, Challenges and prospects. In *Biodiesel-Feedstocks, Production and Applications*; Fang, Z., Ed.; InTech, 2012.
[8] Agarwal, A. K.; *Prog. Energy Combust. Sci.* **2007,** *33*, 233-271.
[9] Awogbemi, O.; Kallon, D. V. V.; Aigbodion, V. S.; Panda, S. *Case Stud. Chem. Environ. Eng*. **2021,** *4*, 100158.
[10] OECD-FAO Agricultural Outlook. OECD Agriculture Statistics (Database). https://reliefweb.int/report/world/oecd-fao-agricultural-outlook-2023-2032?gad_source=1&gclid=EAIaIQobChMIqoGfn8aThgMVC6ZmAh3ssgSyEAAYASAAEgKX3_D_BwE (accessed March 11, 2024).
[11] Aleman-Ramirez, J. L.; Okoye, P. U.; Torres-Arellano, S.; Paraguay-Delgado, F.; Mejía-López, M.; Moreira, J.; Sebastian, P. J. *Fuel* **2022,** *324*, 124601.
[12] Aleman-Ramirez, J. L.; Moreira, J.; Torres-Arellano, S.; Longoria, A.; Okoye, P. U.; Sebastian, P. J. *Fuel* **2021,** *224*, 118983.
[13] Aleman-Ramirez, J. L.; Okoye, P. U.; Pal, U.; Sebastian, P. J. *Renew. Energy* **2024,** *224*, 120163.
[14] Selaimia, R.; Beghiel, A.; Oumeddour, R. *Procedia-Soci. Behavior. Sci.* **2015,** *195*, 1633-1638.
[15] Yusuff, A. S.; Gbadamosi, A. O.; Popoola, L. *J. Environ. Chem. Eng*. **2021,** *9*, 104955.
[16] Ahmad, R. M.; Zafar, M. *Mater. Today Commun*. **2023,** *35*, 105611.
[17] Degfie, T. A.; Mamo, T. T.; Mekonnen, Y. S. *Sci. Reports* **2019,** *9*, 18982.
[18] Park, S. H.; Khan, N.; Lee, S.; Zimmermann, K.; DeRosa, M.; Hamilton, L.; Hudson, W.; Hyder, S.; Serratos, M.; Sheffield, E.; Veludhandi, A.; Pursell, D. P. *ACS Omega* **2019,** *4*, 7775-7784.

[19] Patil, U. P.; Patil, R. C.; Patil, S. S. *J. Heterocyclic Chem.* **2019,** *56*, 1898.
]20] Patil, U. P.; Patil, R. C.; Patil, S. S. *React. Kinet. Mech. Catal*. **2020,** *129*, 679.
[21] Patil, U. P.; Patil, R. C.; Patil, S. S. *Org. Prep. Proced. Int*. **2021,** *53*, 190.
[22] Patil, U. P.; Patil, S. S. *Top. Curr. Chem*. **2021,** *379*, 36.
[23] Patil, U. P.; Patil, S. U. *Indian J. Chem. Technol.* **2023,** *30*, 265-277.
[24] http://hdl.handle.net/10603/337828 (accessed March 11, 2024).
[25] Patil, U. P. *Chinese Chem. Lett.* **2024,** *35*, 109472.
[26] Orwa, C.; Mutua, A.; Kindt, R.; Jamnadas, R.; Simons, A. *Agroforestree Database: A Tree Reference and Selection Guide Version 4.0*; World Agroforestry Centre, Kenya, 2009.
[27] https://indiabiodiversity.org/species/show/228759 (accessed March 11, 2024).
[28] https://www.nutrition-and-you.com/custard-apple (accessed May 4, 2024).
[29] Zahid, M.; Mujahid, M.; Singh, P. K.; Farooqui, S.; Singh, K.; Parveen, S.; Arif, M. *IJPSR*. **2018,** *9*(5), 1-7.
[30] XRD Crystalline (grain) Size Calculator (Scherrer Equation)-InstaNANO. https://instanano.com/all/characterization/xrd/crystallite-size/ (accessed May 4, 2024).
[31] Hammett, L. P. Deyrup, A. J. *J. Am. Chem*. *Soc.* **1932,** *54*, 2721.